

Study of The Spatio-Temporal Relationship Between VIIRS and LiDAR Satellites Imagery of Sulfur Dioxide Emissions from Mergeb Cement Plant in Khums City, Libya

Dawi Muftah Ageel*

Department of Earth & Environmental Sciences, Faculty of Science, Elmergib University, Khums, Libya.

*E-mail: al_ag2008@yahoo.com

دراسة العلاقة المكانية والزمانية بين صور سواتل VIIRS و LiDAR لانبعاثات ثاني أكسيد الكبريت من مصنع إسمنت المرقب في مدينة الخمس، ليبيا

الضواوي مفتاح عقيل*

قسم علوم الأرض والبيئة، كلية العلوم، جامعة المرقب، الخمس، ليبيا.

Received: 4 November 2019; Revised: 16 December 2019; Accepted: 20 December 2019

Abstract

Mergeb Cement Factory is a negative environmental phenomenon due to gas emissions, including sulfur oxides emissions. In this study, the visible infrared imaging group (VIIRS) and LiDAR satellite data were used to determine the similarity in spatial and temporal distribution and intensity of sulfur dioxide emissions. The similarity of the sulfur dioxide emissions distribution during the study period from 2010 to 2017 was shown to analyze the sulfur dioxide emissions in Mergeb factory in Khums, Libya. The results proved that VIIRS and LiDAR observations accurately show the spatial variability in the emission center which was also characterized by heterogeneity in the areas surrounding the plant at concentrations of 0.2 to 1.3 Tons per year according to LiDAR sensor observations and compared with VIIRS sensor concentrations were 0.1 to 1.9 Tons per year. The comparison of VIIRS techniques with LiDAR probes showed a strong positive correlation between the sensors in calculating the values of these emissions.

Keywords: VIIRS, LiDAR, SO₂ emissions, Mergeb, Libya.

الملخص

يمثل مصنع المرقب للإسمنت ظاهرة سلبية على البيئة بسبب انبعاثات الغازات ومن ضمنها انبعاثات أكاسيد الكبريت، استخدمت في هذه الدراسة مجموعة الإشعاع المرئي للتصوير بالأشعة تحت الحمراء (VIIRS) وبيانات القمر الصناعي LiDAR المستخدمة في هذه الدراسة لمعرفة مدى التشابه في التوزيع المكاني والزمني وكثافة انبعاثات ثاني أكسيد الكبريت. أوضحت التشابه الكبير لتوزيعات انبعاثات ثاني أكسيد الكبريت خلال مدة الدراسة من عام 2010 إلى عام 2017 لتحليل انبعاثات ثاني أكسيد الكبريت في مصنع المرقب بمدينة الخمس، ليبيا. أثبتت النتائج أن رصدات VIIRS و LiDAR توضح بدقة التباين المكاني في مركز الانبعاثات التي تميزت بعدم تجانسها كذلك في المناطق المحيطة بالمصنع وبتراكيز 0.2 إلى 1.3 طن سنويا حسب مشاهدات المتحسس LiDAR ومقارنة مع المتحسس VIIRS كانت تراكيز الانبعاثات 0.1 إلى 1.9 طن سنويا، ومقارنة تقنيات VIIRS بتحقيقات المتحسس LiDAR أكدت على وجود علاقة طردية قوية بين المتحسسين في حساب قيم تلك الانبعاثات.

الكلمات الدالة: VIIRS، LiDAR، انبعاثات ثاني أكسيد الكبريت، المرقب، ليبيا.

1. Introduction

Archaeological unearthing includes given away that since About 5600 B.C. In the Mediterranean area, cementation materials were used. For building construction. Now, Portland cement, manufactured during the Industrial Revolution in England and named after the island of Portland in the English Channel, is the most common type of cement. Clinker was burned in dome and shaft kilns in the early days of Portland cement manufacturing, but in the late nineteenth century, these types of furnaces were outstripped by the revolving oven, which has since been the preferred way to make cement clinker (Miller and Hansen, 2004). At the beginning of the current cement production. The generation of facilities grew larger. Also, the impact on the environment, especially on the restricted population has significantly expanded. Since the 1970s, the production of toxic gasses has been a problem for the cement industry (Huntzinger and Eatmon, 2009).

Combined with more knowledge of what harmful gas emissions can do to humans, the number of confined components has increased while emission limits have been set. The uprising focused on environmental aspects forced producers of cement to fix pollution problems. While the provision of heap and efficient treatment emission equipment is an important area for equipment suppliers (Miller and Hansen, 2004).

Predicting pollution has also become more important as new plants, as well as recreational breathing plants, are often expected to be transported with the guarantee that cement and cement processing will be achieved by the machinery (Huntzinger and Eatmon, 2009). Makes cement one of the world's leading bulk chemicals. Cement is produced in most countries due to the abundance of raw resources. Cement processing is a highly energy-intensive process and the sector absorbs 2% of the world's energy and transmits 5% of man-made SO₂ emissions (Finus, 2003). Reducing SO₂ emissions has been a critical problem for the cement industry for several years. Throughway of the need for wisdom and techniques for spreading SO₂ emissions without movement due to tighter and tighter impediments to emissions. In Europe and North America in particular, the 2008 report from the Environmental Protection Agency (EPA) for application (Li *et al.*, 2005.a). Recommend 0.6 kg SO₂ per ton of clinker control. Coming in vegetation in a line by means of a high sulfur satisfy in inexperienced materials anticipating to use 5-7% of clinker costs to distribute the expected restrictions. In a cement plant, SO₂ starts from both raw and expanded supply. In each of the oven burner or calciner, the SO₂ from the fuel is released. In any case, SO₂ starting from the oil does not produce a pollution problem in conjunction with depleted gas, because the calciner and the bottom twister act as dry scrubbers, which customarily strip off SO₂ from the fuel entirely. SO₂ from the raw meal mainly develops in the preheater tower through the oxidation of pyrite and organic sulfur impurities, with most of the sulfur being found as pyrite inclusions (Li *et al.*, 2005.b). The oxidation of sulfur species begins between 300-600°C, corresponding to the two peak tornado in a preheater of the sulfur that comes in during the raw meal, it is frequently accepted to exceed 50% because SO₂ (Mateshvili *et al.*, 2013). The amount can vary from 10 to 65 percent in any case, resulting in seriously mistaken estimates

of SO₂ emissions as an effect. Winker *et al.* (2003) reported that an increased number of cyclone stages in the preheater tower also increased SO₂ emissions based on plant emission data, What they clarified by establishing that when the number of cyclone stages increases, less CaO comes to the top stages. Bauer *et al.* (2009) investigated the decay of pyrite. Who establishes that pyrite can break down in an oxygen-containing atmosphere by direct corrosion or warm degradation of pyrite and sulfur, accompanied by successive oxidation of SO₂ and iron oxides. At temperatures below 525°C, the ruling mean will be 3.1 if the concentration of O₂ is sufficiently high; otherwise, reaction 3.2 will dominate the creation of SO₂ (Miller and Hansen, 2004).

1.1.Sulfur Dioxide Reduction in Cement Plants:

Methods for reducing SO₂ emissions from cement plants have been an issue for years, at some point in which a well-constructed number of patents and obvious applications are submitted, with different approaches to highlighting SO₂ emission problem in cement manufacturing (Johansen *et al.*, 2016). The methods are divided into three categories by Cem bureau. Precursor discount if the emission precursor is reinforced in the kiln system, emissions will be reduced as a natural consequence. This can be achieved by extracting beautifully areas with a high ancestor content in the prey (Greer *et al.*, 2010). Another plausibility is to replace some with one or more raw resources that restrict fewer herald emissions. Generally speaking, reducing the precursor can be a practically cheap way to address emission issues. However, if the ancestor is equally transported and established in one of the primary raw materials, this means is not suitable (U.S. Environmental Protection Agency, 2005).

Primary methods of lessening, these approaches include structures where pollution problems are unraveled by making a slight change to the living system so that interest is introduced in the way. Miller and Hansen (2004) outlined some of the main methods that can be used, such as using a calciner trip brook whereby a fraction of the calciner content is recycled to the pinnacle phases of the preheated SO₂ surpass in charge. By action, a 25-30 percent reduction in SO₂ can be achieved after approximately 5 percent recycling of the calciner material. Adding hydrated emerald to the pinnacle stages of the preheater loom is another major reduction method, capable of reducing SO₂ emissions by 45-70% .

Hydrated lime costs, however, make the operating costs relatively high. To handle the high cost of materials. Secondary decrease strategies: these are techniques that rely on technology that has been introduced as dividing units to spread emission problems. Secondary bases have the advantage that flow reduction is very high, often more than 90 percent, which is why a secondary decrease process can be central if emission issues are plain. But, fundamental methods of decrease or precursor discount are easiest (Miller *et al.*, 2001).

Visible Infrared Imaging Radiometer Suite (VIIRS) used one of the most commonly used data to interpret some economic-environmental issues, like greenhouse gases. Images of the Earth at Night, taken from nighttime satellite images given by Visible Infrared Imaging Radiometer Suite (VIIRS), are now an identifiable spatially honest worldwide idolization of biological participation on a planet (Wolfe *et al.*, 2013).

VIIRS values for the SO₂ distribution analysis are compatible with the measurement of thermal emissions from quarry plants. SO₂ emissions have grown to be one of the most critical problems facing all countries in the world for sustainable development. More than 70% of total greenhouse gas emissions were contributed by fossil fuel-related SO₂ emissions, which have a profound effect on physiological, biological systems such as climate change, rising sea levels, loss of biodiversity, declining agricultural productivity (Cao *et al.*, 2013).

Earlier studies have shown that SO₂ emissions can be estimated using VIIRS at the 1-km spatial height. Emissions of SO₂ in unlit pixels, for instance, could be absent; emissions could be underestimated due to the saturation area; whereas emissions in areas far from the source could be measured downwards. However, in previous studies on this site, the same method of measuring SO₂ emissions is not available. Sulfur dioxide (SO₂) is formed by thermal deterioration in the clinker of calcium sulfate and indicates the temperature of the clinker (Pugnaghi *et al.*, 2006). SO₂ is available and broken down to SO and O₂ as anhydrite. Remote sensing methods are important to track the atmosphere of the earth. In atmospheric backscattering experiments, air emission was analyzed using laser techniques. Due to its unique nature and enormous adaptability, the laser radar or lidar approach offers particular advantages. Pulsed laser light is transmitted to the atmosphere and light from particles and aerosols is collected and analyzed by an optical telescope (Eckhardt *et al.*, 2008).

In addition to data on particle content, details of the 3D distribution of certain molecular contaminants can be obtained using the so-called knob technique (differential absorption lidar). The particle back dispersion is measured for two electromagnetic radiations, where the gas to be investigated strongly and weakly absorbs (Garland *et al.*, 2008).

2. Methods

2.1. Study Area

Khums city located in the western north part of Libya between Longitude 14°37'51"E and Latitude 32°35'26"N (Figure 1), and surrounded by the capital (Tripoli, 130 km west), Misurata city (82 km east), with area 1,594.2 km² and bordered by Mergeb plains in the south with coordinates 32°38'13" N and 14°13'27" E, which rises from 84 to 127 meters from the sea, with population average reach to 453,297 people according to 2012 statistics. Different in the proportions of their distributions per kilometer, which increases this proportion as approach the center of the city.

The cement plant and it Kaolinite quarry (it is the main material for the cement industry) is located close to the urban area of Khoums city about six kilometers from the entrance to the city center, which poses a greater danger to the residents of the city. The factory and the quarry are located on an area be rich in plant diversity. It is full of olive trees, which is also pastoral areas.

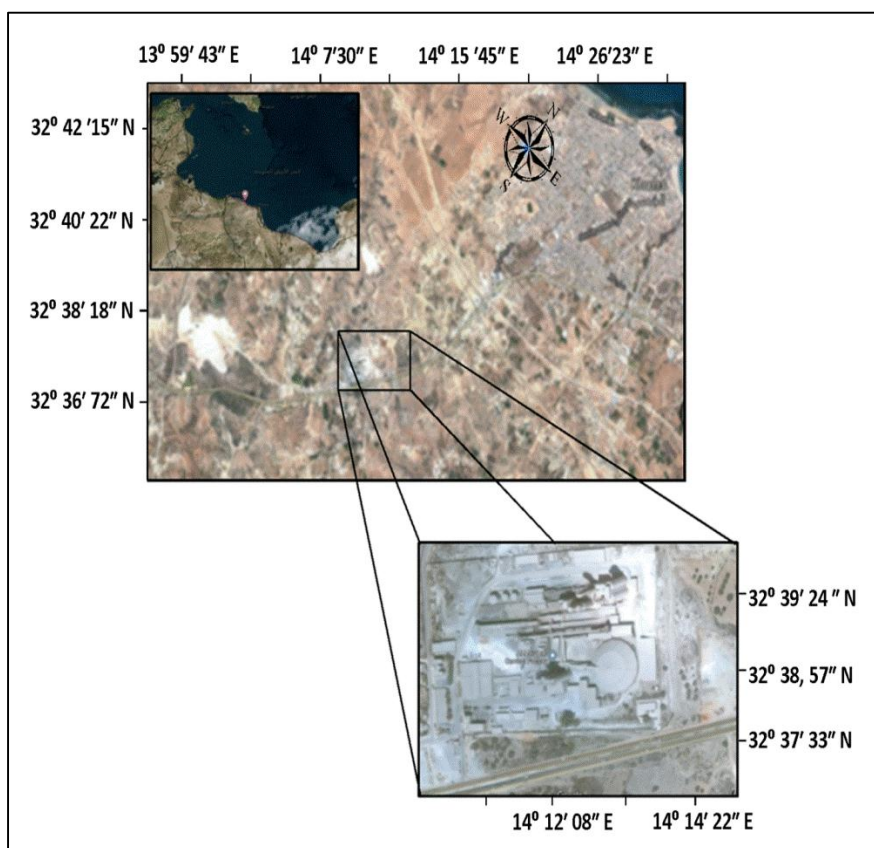


Figure1. Study area with cement plant location

2.2. Sulfur Dioxide Data by (VIIRS) Imagery

A component of the satellite of the Suomi National Polar-orbiting Partnership (NPP) is the Visible Infrared Imaging Radiometer Suite (VIIRS) instrument. Suomi NPP, including VIIRS. To develop and launch the next generation of polar-orbiting satellites, the Joint Polar Satellite System (JPSS), a joint NOAA/NASA project, was developed. The VIIRS sensor was designed to extend and enhance the Advanced Very High-Resolution Radiometer (AVHRR) series of measurements initiated by its predecessors. The Moderate Imaging Spectroradiometer (MODIS) and the Seawide Field of View Sensor (SeaWiFS) resolution (Wang *et al.*, 2005).

The instrument VIIRS is a radiometer of whisk broom with 22 channels ranging from 0.412 μm to 12.01 μm . Five of these channels are image bands or I-bands with high resolution, sixteen are designed as moderate-resolution bands or M bands, as they are commonly called. One of these M-bands is the day/night band, or DNB, which is a sensitive panchromatic band to visible and near-infrared wave lengths. With this unit, VIIRS will track nighttime lights on Earth using greater spatial and temporal resolution than its predecessors. VIIRS data used in this analysis to calculate. Mergeb cement plant SO_2 gas emissions (Blonski *et al.*, 2014).

2.3. Sulfur Dioxide Data by LiDAR Imagery

The acronym lidar engineering for light detection and ranging (Lidar) stands for light detection and scope. There are many parallels with radar in this design. A brief light pulse is released. Molecules and aerosols in the atmosphere reflect some of the light. This reflected light is obtained, measured and analyzed with a telescope. The distance to the reflecting particles to the Lidar can be derived by measuring the time elapsed between sending and receiving the light. The identified Lidar is mounted on a vehicle. This Lidar unit sends out two light pulses of different colors in a short series (Lefsky *et al.*, 2002).

The colors are picked in such a way that the target gas (in this case SO₂) absorbs the first color more intensely than the second color. When SO₂ is present, the light will be reflected. From the first light pulse, the light from the second pulse will be more heavily attenuated. The concentration of SO₂ can be determined from the degree of attenuation at the place where the light is reflected. Because light reflecting molecules are everywhere along the light beam path (Eitel *et al.*, 2016).

Imagine the cloud aerosol Lidar with spectral orthogonal polarization. LiDAR data used to detect three channels (532 nm parallel, 532 nm perpendicular, 1064 nm) elastic LiDAR light receiving the same wavelength as the laser frequency emitted. LiDAR sends downward to earth short and intense pulses (1064 and 532 nm) of linearly polarized laser light. The atmospheric backscatter profile is obtained from 8 to 20 km with a horizontal resolution of 1 km at 60 m vertical resolution (Bergen *et al.*, 2009).

Together with the Atmospheric Science Data Center (ASDC) at NASA Langley Research Center and HYGEOS/AERIS/ICARE Data Center and Services Center, the CALIPSO mission team announces the launch of an upgrade to the Generic Level 2 LiDAR data items.

The products of V4.20 CALIOP Level 2 contain new data sets of laser energy science. A technical advice on this phenomenon and recommended ways to mitigate its impact on scientific analysis. It was noted that the current V4.10 CALIOP Level 2 data set did not contain sufficient information to classify low energy shots without accessing the correct V4.10 CALIOP Level 2 files (Pelon and McCormick, 2003).

The new V4.20 CALIOP Level 2 files now include science data sets for both 532 nm single-shot energy (directly from the Level 1 product) and a minimum of 532 nm laser energy per 80 km chunk to provide a simpler method of excluding affected level 2 data. This avoids the need to download both the data products of CALIOP Level 1 and Level 2 to exclude the profiles affected. All other V4.20 Level 2, science data sets are identical to V4.10 Level 2 products (Hunt and McGill, 2007).

2.4. Wind speed and Wind Direction Measurements

Sentinel (1) satellite (Synthetic Aperture Radar (SAR)) data from the European Remote Sensing Satellite (ERS) were used to map wind speed and wind direction to understand wind fields around Mergeb cement plant's SO₂ emissions. This method for deriving Sentinel

Synthetic Aperture Radar (SAR) data from 500 m resolution wind speed maps (Hees *et al.*, 2011).

2.5. Static Analysis:

For two cases, regression analysis is used to compare producers between two variables, namely SO₂ emissions from cement plume and length of SO₂ plume distributions for different terms, using this static equation (Aldrich, 2005):

$$y = d + \frac{a-d}{1+\left(\frac{x}{c}\right)^b} \dots\dots\dots (1)$$

where:

y : depends on the independent variable

$d + \frac{a-d}{1+\left(\frac{x}{c}\right)^b}$: the slope form of the linear equation

x : the independent variable

3. Results

3.1. Spatial Distributions of SO₂ Emissions by VIIRS Imagery

The results found that SO₂ emissions mainly concentrated in the center of the plume. Visually, the SO₂ emission density in The night-time is higher than the day. The highly concentrates including August 2012, May 2015 and June 2017. SO₂ values recorded as ranged from 0 to 93 (kg/month). The SO₂ emissions density to every month have range from 13 to 28 (kg/month), has more than doubled from 23 to 87 (kg/month) between 2012 and 2017. While highest brightness recorded in 2010, 2012, 2013 respectively.

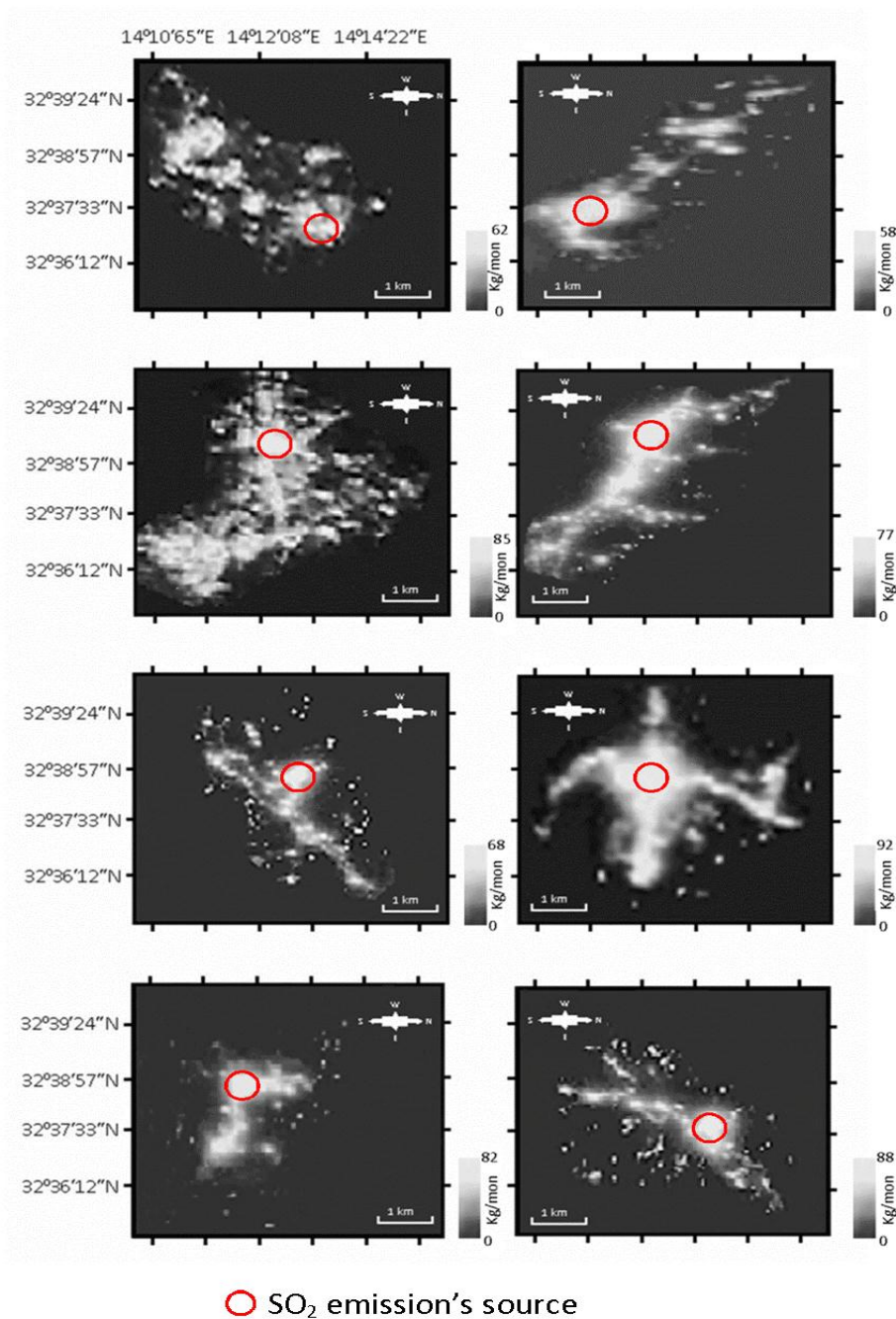
By aggregating the pixel level of SO₂ emissions to the plumes and examining the Spatio-temporal characteristics, it was noted that the results of the correlation between satellite data during the study period were significantly positive, suggesting that the spatial distribution of SO₂ emissions during the study period were identical. The ILWIS 3.8 used for the spatial Analysis to the hot spots of plume pollution incidents, and eight-time points in 2010, 2013, and 2015, and 2017 were selected for the comparative analysis.

VIIRS classification which determines the best value arrangements in different brightness and aims at showing variance in classes and optimizing variance in SO₂ emissions.

The spatial agglomeration levels of SO₂ emission incidents were classified from high to low as very thick spot agglomeration areas, thick spot agglomeration areas, medium spot agglomeration areas. Rare-spot areas of agglomeration and non-spot areas of agglomeration, respectively. Eventually, the spatial and temporal trends of incidents of SO₂ emissions at the cement plant in Mergeb have been identified and shown in Figure (2).

According to the observations described down, the spatial distributions of eight SO₂ emission from cement plant emissions were derived from VIIRS data. The SO₂ emission images from VIIRS data from 2015 to 2017 had a spatial resolution of more than the years 2010 to 2014 of about 1 km. As shown in Figure (2), all SO₂ concentrations during the study

period were dispersed in all plumes directions, affected by weather conditions, production effort and lack of filters in factory chimneys.



○ SO₂ emission's source

Figure 2. The common monthly spatial patterns of SO₂ emissions by VIIRS during of the study period.

During most of the study period, high concentrations are typically aggregated in the central area of the SO₂ plume, and summer plumes occurred in the south-eastern part of SO₂ emissions. While low concentrations in the western and northern parts of the SO₂ plumes appeared in winter plumes. The wind direction influenced the concentrations of SO₂, wind

stress and brightness degree of the light as shown in Figure (4). Where SO₂ distributions separated by seasons have been shown; (a) Winter (b) Spring (c) Summer (d) Autumn. There were relatively low annual and seasonal average concentrations of SO₂ emissions. From a spatial perspective, it is necessary to know the characteristics of SO₂ emissions. It is essential to quantify the spatial patterns of plumes in an industrial area for a long time in order to investigate the air environmental quality in this area.

3.2. Spatial Distributions of SO₂ Emissions by LiDAR Imagery

The data required to verify spatial similarity with LiDAR results. SO₂ emissions can be grouped into five wavelengths. In this section VISAT analysis used to measure the spatial pattern of SO₂ concentrations annually. Figure (3) shows spatial data of SO₂ emissions included in layers in the frame of a VISAT project. Where the red band represents SO₂ concentrations that resulting from cement plume. While yellow and green bands were given a gradual reading to SO₂ concentrations, the least was when the green band until SO₂ concentrations were non-existent in blue band.

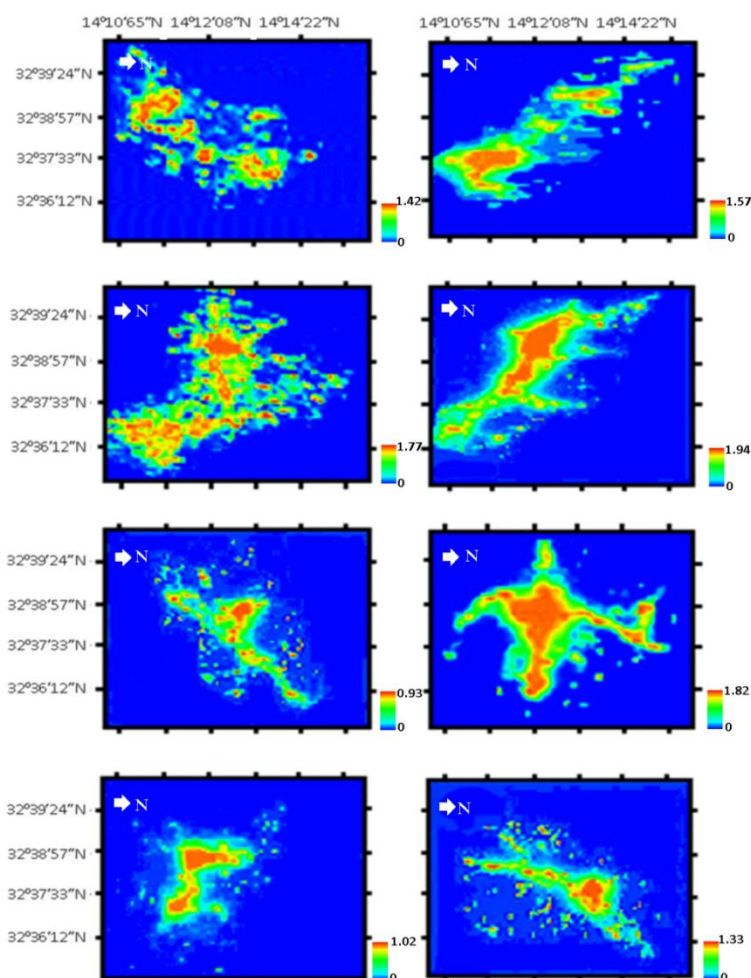


Figure 3. The common annual spatial patterns of SO₂ emissions by LiDAR during of the study period.

Mergeb cement plant area has maintained relatively low annual and seasonal average concentrations of SO₂ emissions. From a spatial perspective, it is necessary to dig further characteristics of these air pollutants. It is essential to quantify spatial patterns of air pollution in an urban area for a long time in order to investigate the air quality in this area. They play an important role in dissipating SO₂ emissions for wind scale and rainfall.

Different wind patterns have different effects on wind direction: Southern winds usually have positive effects, while northern winds have negative effects on SO₂ ratios. Regarding the impact of wind direction SO₂ concentrations, high concentrations (from 12 to 15 mile per hour) were mostly aggregated in the northwestern, western winds while low concentrations (from 5 to 7 mile per hour) were aggregated in the southern and eastern winds. The main source of SO₂ was usually emissions from Mergeb cement plant.

Appropriate research found that the wind direction had a significant impact on the air production of SO₂ (Figure 4).

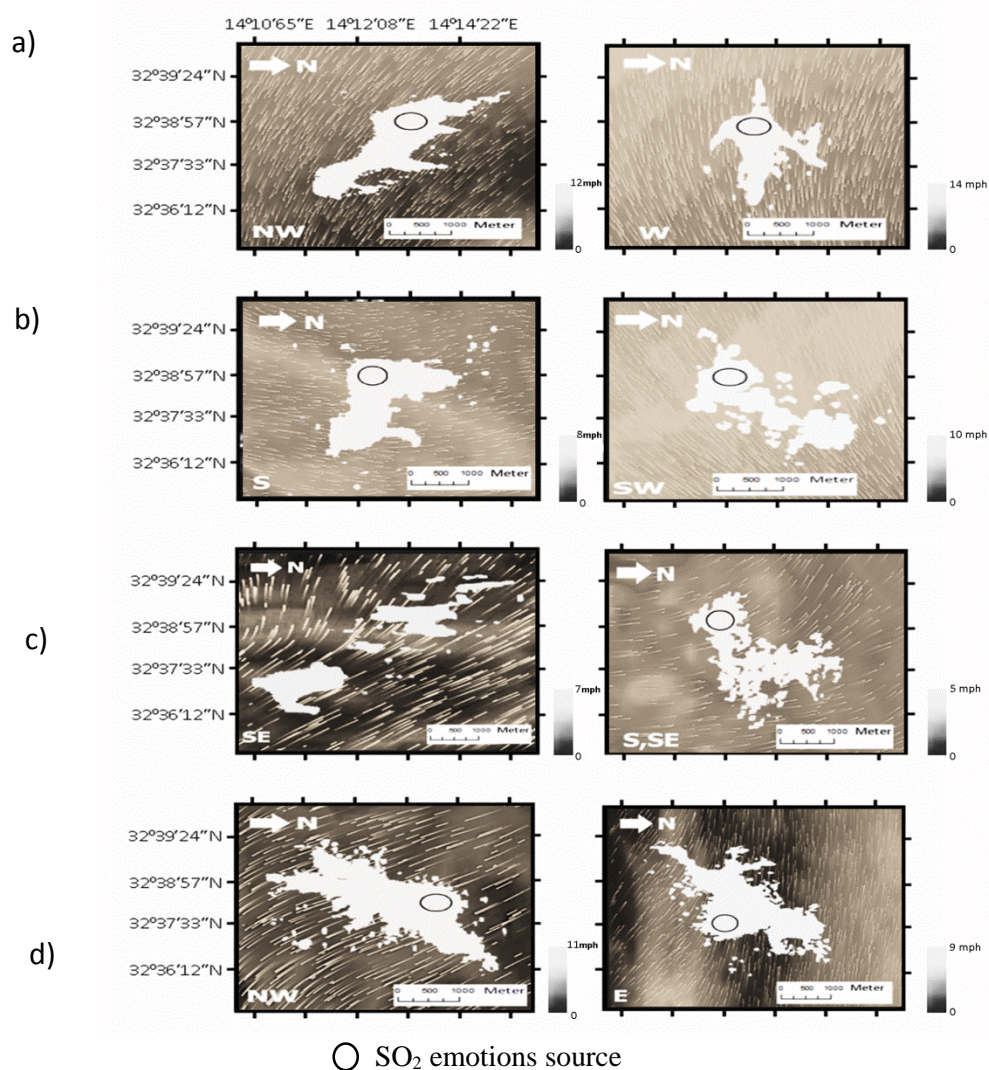


Figure 4. Showing four seasons represents wind speed occur as clouds and wind direction and their influence on SO₂ distributions during study period, (a) Winter season, (b) Summer season, (c) Autumn season, and (d) Spring season.

4. Discussion

4.1. Regression Analysis:

For determine the relationship between VIIRS and LiDAR observations, these results were compared using regression analysis, the comparison was during the selected years, the aim of the study can be checked for robustness and reliability.

As shown in Figure (5), even the same sensor had large differences in each year, winter and spring seasons value were smaller than from Summer and Autumn seasons value to VIIRS and LiDAR data during of study period.

The main reason for these differences could be the different scope of VIIRS accounting. VIIRS accounted for SO₂ emissions from industrial processes in the last few years, while VIIRS accounted for low levels in the early years. Regardless, the results are similar to each other, were is proven that the relationship between VIIRS and LiDAR data was strong positive($r^2=94$), as shown below (Figure 5).

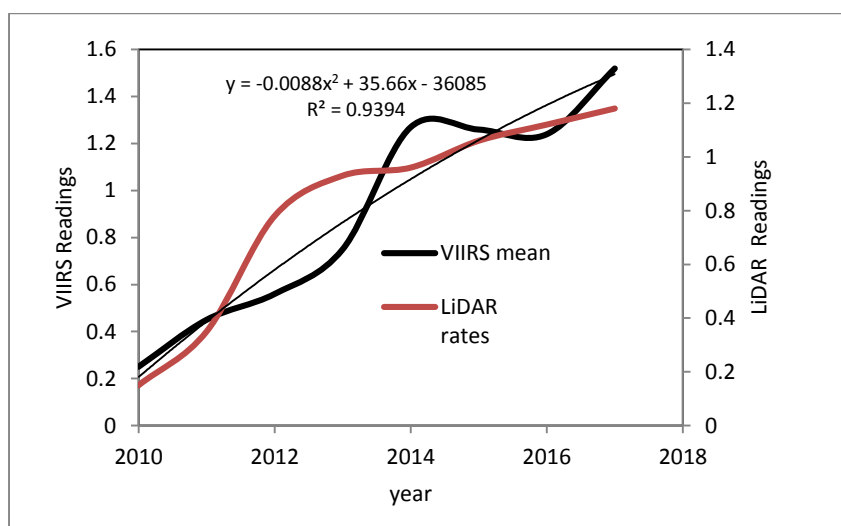


Figure 5. Comparison of the annual relationship of SO₂ emissions between LiDAR and VIIRS observations.

Figure (6) showed that the more from the gas cement plume spread, SO₂ concentration was less. This deployment of the concrete plume depends on the amount of output and the wind speed.

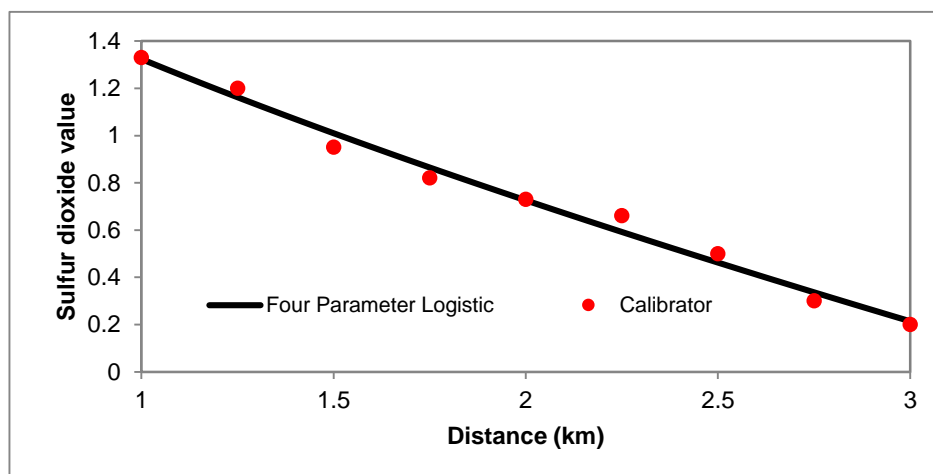


Figure 6. Reverse relationship between sulfur dioxide concentrations and spread distance of the concrete plume.

From the figure above there is a strong reverse relationship ($R^2 = -0.68$). Although the proposed methods have proven effective and accurate in analyzing the problem of SO_2 emissions. There are many limitations in the future study that can be improved. Because of air borne dust or water vapor, it took into account information distorted from spatial images of SO_2 emissions to enhance VIIRS performance. Because of the global coverage of VIIRS and SO_2 emissions and the growing availability of spatial information for gas emission and temperature changes and ambient humidity with resolution of 1 km and 30 m (Lihang *et al.*, 2019).

The methods proposed could also be applied to other countries and regions and other environmental issues, such as the distribution of steel stocks in human society and the consumption of residential energy. The improved accuracy and sensitivity of SO_2 measurements from LiDAR and VIIRS sensors allow SO_2 cloud mapping and long-range monitoring, but the identification of large amounts of SO_2 in cement plumes still presents many challenges. These include the potential effects on birds and air crafts of elevated levels of SO_2 , sulfate aerosol, and other acid gases in ash-poor clouds. It is well known that SO_2 and ash components can be separated in gas clouds and can travel in different directions depending on the wind shake (Schueler *et al.*, 2013). It is therefore important to track SO_2 in order to obtain a complete picture of the risk of emissions. Although SO_2 is transmitted to the surface water, soil and vegetation are definitely more damaging, more work with other remote sensors on the potential effects of SO_2 , other acid gases and acid aerosol experiments on cement plumes urgently needed in the future. Work has been done on the effects of SO_2 on soils, water, and air which during the study period may have implications for the actions of the local environment. More research is warranted by the possible effects of sulfur dioxide. An important step towards clarifying the concentrations and distributions of sulfur dioxide is the analysis of SO_2 emission through LiDAR and VIIRS sensors.

5. Conclusion

Mergeb cement plant was selected as a case to SO₂ emissions and to increase understanding of its Spatio-temporal variations of SO₂ emissions from 2010–2017. VIIRS can give more information about SO₂ emissions in air using radiance of the night light, which cannot imagery in another way in the night. Second, this imagery was compared by LiDAR satellite that specialist in gas emissions observation. Third, the results show great potential to be applied further as a proxy for many environmental and pollution problems, particularly in regions lacking sufficient and reliable statistical data. Forth, it is observed that the concentration of emissions sulfur dioxide was higher in the area around the plant than in other areas.

These results provide guidance for decision-making in implementing sustainable development strategies and low sulfur policies. Although the approaches suggested have proven efficient and reliable in evaluating the issue of SO₂ pollution, in the future study there are many weaknesses that can be improved. First, due to atmospheric dust, water vapor or poor night light did not take into account the lack of clarity of data from spatial images of S O₂ emissions. More efforts should be made to improve data quality and to integrate more variables into the analytical algorithms used for advanced space images of particular importance is the fact that sulfur dioxide emissions are not only responsible for the source but also by factors such as the degree of wind stress and direction and poor urban and agricultural planning around the source environment.

References

- Aldrich J. (2005). Fisher and regression. *Statistical Science*, 20(4): 401-417.
- Bauer K., Thormann J, and Lohnherr L. (2009). Method of removing sulphur dioxide from cement kiln exhaust gases. *Environ. Sci. Technol. J.*,15: 43-92.
- Bergen K.M., Goetz S.J., and Radelof V.C. (2009). Remote Sensing of vegetation 3-D structure for biodiversity and habitat: review and implications for LiDAR and radar space borne missions. *J. Geophys. Res.*, 12:114-123.
- Blonski S., Cao C., Shao X., and Uprety S. (2014). VIIRS reflective solar bands calibration changes and potential impacts on ocean color applications. In: *Ocean Sensing and Monitoring VI*. International Society for Optics and Photonics, 9111: 91-111.
- Cao C., Xiong J., Blonski S., Liu Q., Uprety S., Shao X., Bai Y., and Weng, F. (2013). Suomi NPP VIIRS sensor data record verification, validation, and long-term performance monitoring. *J. Geophys. Res.*, 11: 664–678.
- Eckhardt S., Prata A.J., Seibert P., and Stohl A. (2008). Estimation of the vertical profile of sulfur dioxide injection into the atmosphere using satellite column measurements and inverse transport modeling. *Atmos. Chem. Phys.*, 3: 81–97.
- Eitel J., Höfle B., Vierling L.A., and Magney T.S. (2016). Beyond 3-D: The new spectrum of LiDAR applications for earth and ecological sciences. *Remote Sens. Environ.*, 8: 372-392.
- Finus M. (2003). International Cooperation to Resolve International Pollution Problems. *EOLSS. J.*, 3(2): 112-148.

- Garland C., Nibler J., and Shoemaker D. (2008). Spectroscopy in Experiments. *Physical Chemistry J.*, 11: 28-39.
- Greer W.L., Dougherty A., and Sweeney D.M. (2010). *Air Pollution Engineering Manual Portland Cement*, Second Edition, Editor: Davis W.T., John Wiley & Sons, Inc., New York, USA.
- Hees A., Grafmüller B., Koch P., Huchler M., Croci R., Østergaard A. (2011). The GMES Sentinel-1 Antenna Model. *The Netherlands J.*, 5(3): 18-21
- Hunt W.H., and McGill M.J. (2007). Initial performance assessment of CALIOP. *Geophys. Res. Lett.*, 3(2): 21–38.
- Huntzinger D.N., and Eatmon T.D. (2009). A life-cycle assessment of Portland cement manufacturing: comparing the traditional process with alternative technologies. *Journal of Cleaner Production*, 17: 68–75.
- Johansen V., Egelov A., and Eirikson A. (2016). Emission of NO_x and SO₂, From Cement Clinker Burning Installations. *Zement-KalkGips NOx 10*: 273.
- Lefsky M.A., Cohen W.B., Parker G.G., and Harding D.J. (2002). LiDAR remote sensing for ecosystem studies. *Bioscience J.*, 5(2): 19–30.
- Lihang Z., Murty D., and Mitch G. (2019). An Overview of the Science Performances and Calibration/Validation of Joint Polar Satellite System Operational Products. *Remote Sens*, 11(6): 87-98.
- Mateshvili N., Fussen D., Mateshvili G., Mateshvili I., Robert C., and Dekemper E. (2013). Nabro volcano aerosol in the stratosphere over Georgia, South Caucasus from ground based spectrometry of twilight sky brightness. *Atmos. Meas. Tech.*, 6: 63–76.
- Miller F.M., Young G.L., and von Seebach M. (2001). Formation and Techniques for Control of Sulfur Dioxide and Other Sulfur Compounds in Portland Cement Kiln Systems, *R and D Serial*, 24(2): 24-56.
- Miller S., and Hansen J. (2004). Methods for reducing SO₂ emissions. *Cement Industry Technical Conference, IEEE-IAS/PCA*: 79-92.
- Pelon J., and McCormick M.P. (2003). The CALIPSO mission: Space borne lidar for observation of aerosols and clouds. *Lidar Remote Sensing for Industry and Environment Monitoring. International Society for Optical Engineering*, 3: 61–86.
- Pugnaghi S., Gangale G., Corradini S., and Buongiorno M.F. (2006). Mt. Etna sulfur dioxide flux monitoring using VIIRS data and atmospheric observations. *J. Volcanol. Geotherm. Res.*, 15(2): 74–90.
- Schueler C.F., Lee T.F., and Miller S.D. (2013). VIIRS constant spatial resolution advantages. *International Journal of Remote Sensing*, 34: 576-577.
- US Environmental Protection Agency (2005). *Compilation of Air Pollutant Emission Factors*. Publication AP-42. Fifth Edition. Volume I - Stationary Point and Area Sources. Research Triangle Park: 346.
- Wang M., Knobelspiesse K., Charles R. (2005). Study of the Sea-Viewing Wide Field-of-View Sensor (SeaWiFS) aerosol optical property data over ocean in combination with the ocean color products. *Journal of Geophysical Research-Atmospheres*, 11: 69-102.
- Wolfe R.E., Lin G., Nishihama M., Tewari K.P., Tilton J.C., and Isaacman A.R. (2013). Suomi NPP VIIRS prelaunch and on-orbit geometric calibration and characterization. *J. Geophys. Res. Atmos.*, 18: 8–21.